A model for induced seismicity caused by hydrocarbon production in the Western Canada Sedimentary Basin

Valentina Baranova, Azer Mustaqeem, and Sebastian Bell

Abstract: Over the past three decades, a significant number of small-magnitude and shallow earthquakes have occurred in the Western Canada Sedimentary Basin and are located along its western flank near areas of oil and gas production. One of the better documented examples is the swarm of earthquakes associated with the Strachan field, in the Alberta foothills. A model based on Segall's poroelastic theory is developed to account for the occurrence of earthquakes below the Strachan reservoir. Using this methodology, we show that the earthquake of 19 October 1996, underneath the Strachan field, was most probably triggered by gas extraction. The numerical model also implies that gas extraction would cause subsidence and localized changes in in situ stress magnitudes. There is a strong correlation between rates of production and the number of seismic events, but the onset of major seismic activity postdates the commencement of production by approximately 5 years. Poroelastic modelling can account neatly for this observed delay. The modelled stress changes due to gas extraction point to a regime which favours reverse or thrust faulting that is compatible with stress magnitude measurements in the area. The proposed mechanism involves volume changes which decrease the vertical stress S_v and increase the larger horizontal stress S_{Hmax}. The mean stress increase beneath the reservoir appears to be small, but increasing the deviatoric stress permits Mohr–Coulomb failure. As a result, the initially high rate and long history of gas extraction appear likely to be the main trigger for the seismicity beneath the Strachan field.

Résumé : Au cours des trois dernières décennies, un nombre important de tremblements de terre de faible magnitude et de faible profondeur sont survenus dans le Bassin sédimentaire de l'Ouest du Canada, et localisés le long de son flanc occidental, à proximité de régions productrices de pétrole et de gaz. L'un des exemples le mieux documenté est représenté par le groupe de tremblements de terre associé au champ de Strachan, dans les Foothills de l'Alberta. Un modèle fondé sur la théorie poroélastique de Segall a été élaboré pour expliquer les événements de tremblements de terre sous le réservoir de Strachan. Nous démontrons par cette approche que la cause la plus probable de déclenchement du tremblement de terre du 19 octobre 1996, sous le champ de Strachan, serait l'extraction du gaz. Le modèle numérique révèle en plus que l'extraction du gaz serait responsable d'un phénomène de subsidence et des changements apparus localement dans la grandeur des contraintes in situ. On observe une forte corrélation entre les taux de production et le nombre d'événements sismiques, mais le début de l'activité sismique significative n'a débuté que cinq années approximativement après le commencement de la production. La modélisation poroélastique rend compte nettement de ce délai observé. La modélisation des changements des contraintes engendrés par l'extraction du gaz pointe un régime qui favorise le développement de failles chevauchantes ou inverses, qui est compatible avec les mesures de la magnitude des contraintes dans la région. Le mécanisme proposé implique des changements de volume dont l'effet est d'affaiblir la contrainte verticale S_v et de renforcer la contrainte horizontale S_{Hmax} plus grande. Il semble que l'augmentation de la contrainte moyenne sous le réservoir soit faible, mais l'accroissement de la contrainte déviatorique est suffisante pour provoquer la rupture Mohr–Coulomb. En conclusion, le taux élevé de l'extraction du gaz au début de l'exploitation et sa longue durée nous apparaissent comme la véritable cause du déclenchement de l'activité sismique sous le champ de Strachan.

[Traduit par la Rédaction]

Received April 4, 1998. Accepted August 28, 1998.

V. Baranova,[1] A. Mustaqeem, and S. Bell. Geological Survey of Canada, 3303 33rd Street NW, Calgary, AB T2L 2A7, Canada.

[1]Corresponding author. Present address: 3, 2127 7 Avenue NW, Calgary, AB T2N 0Z8, Canada (e-mail: mustaqea@cadvision.com).

Introduction

In the latter half of this century it has become apparent that certain engineering activities can lead to earthquakes in the upper crust (Gough 1978; Simpson 1986; Knoll 1992; Bell 1996). Generally, these activities are not the sole cause of the earthquakes; they merely induce seismic activity by altering stress regimes, so failure occurs. In effect, these are humanly triggered earthquakes. Triggered seismicity can re-

Fig. 1. Contemporary stress field in the Western Canada Sedimentary Basin.

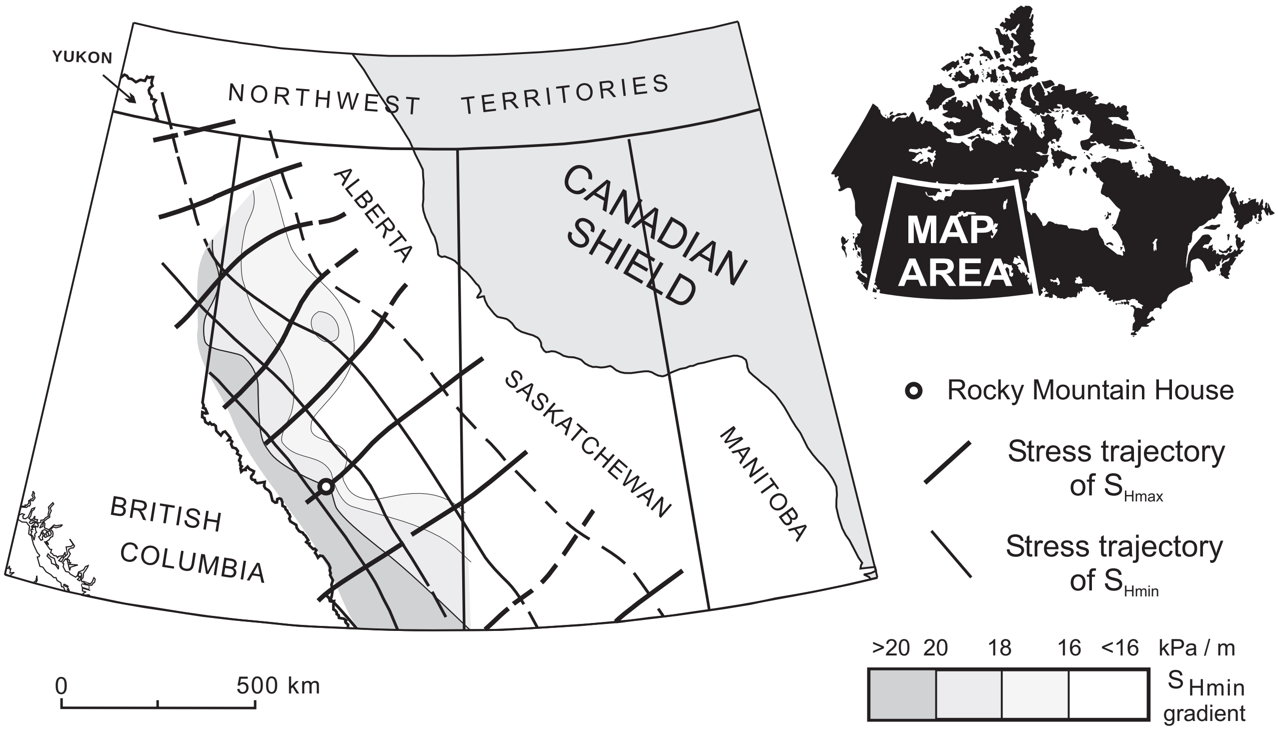

sult from (*i*) impounding of reservoirs (Gough 1970; Bell and Nur 1978; Gupta and Rastogi 1979), (*ii*) quarrying or mining and subsurface extraction of fluids (Pomeroy et al. 1976; Gendzwill et al. 1982; Segall 1989; Davis et al. 1995), (*iii*) subsurface injection of fluids (Healy et al. 1968; Raleigh et al. 1972; Hsien and Bredehoeft 1981; Davis and Frohlich 1993), and (*iv*) underground explosion (Console and Nikolaev 1995). Each of these activities is characterized by specific mechanisms, most of which involve pore-pressure changes (Kisslinger 1976).

The present paper deals with seismicity resulting from fluid extraction. Theoretically, the mechanism involved is similar to that which promotes seismicity during mining activities (McGarr et al. 1975; Pomeroy et al. 1976; Gendzwill et al. 1982). Many authors such as Segall (1985, 1989), Yerkes and Castle (1976), and Smirnova et al. (1975) have proposed different models for this type of triggered seismicity.

The area highlighted in this study lies on the western flank of the Western Canada Sedimentary Basin in Alberta, near the town of Rocky Mountain House (Fig. 1). This is not an area of high natural seismicity (Rogers and Horner 1991), but, over the past several decades, numerous small-magnitude earthquakes have occurred along the western flank of the basin in areas where oil and gas have been extracted (Milne 1970; Milne and Berry 1976; Rebollar et al. 1982, 1984; Wetmiller 1986). Many are suspected to have been triggered by hydrocarbon production, but this is unproven because of lack of on-site monitoring. For example, Milne (1970) described a magnitude 5.1 earthquake that occurred in 1970 at Snipe Lake, Alberta. He noted that its location was anomalous and speculated that its occurrence might be related to oil and gas production activities in the area. Rebollar et al. (1982, 1984) and Wetmiller (1986) investigated earthquake swarms near Rocky Mountain House, Alberta. Wetmiller concluded that the earthquakes may have been induced by gas production. A much stronger case for induced seismicity was made by Horner et al. (1994) for the recent earthquake swarm near Fort St. John, British Columbia, which has been extensively monitored. Horner et al. have assembled stress and fluid-pressure data which suggest that the probable triggering mechanism for these earthquakes is water injection into oil-bearing Permian Belloy Formation sandstones in the Eagle and Eagle West fields.

In this study, we revisit the Rocky Mountain House earthquakes, evaluate their occurrence in the light of gas production from the Strachan field, and propose a mechanism to explain their timing and nature.

Geomechanical setting of the Western Canada Sedimentary Basin

The Western Canada Sedimentary Basin extends along a southeast–northwest-trending axis across southern Manitoba, southern Saskatchewan, Alberta, and northeastern British Columbia (Fig. 1). It contains Phanerozoic sediments ranging in age from Cambrian to Palaeocene which rest unconformably on metamorphic rocks of the Canadian Shield. The Paleozoic section is dominated by carbonates that accumulated in passive-margin environment (Mossop and Shetsen 1994), whereas the overlying Mesozoic and Cenozoic rock units are predominantly clastic and accumulated in a foreland-basin setting (Leckie and Smith 1992). The foreland-basin deposits form a series of west-thickening wedges and, together with the underlying Paleozoic sediments, are overthrust along the western flank of the basin. Total sediment thickness reaches 5 km along the western margin of the basin.

Fig. 2. Seismicity of Alberta (1957–1997) including the location of seismic network. Seismograph stations are as follows: 1, PNT (1960); 2, SES (1966); 3, EDM (1963); 4, BAN (1955–1966); 5, MCC (1966); 6, DOWB (1982); 7, SLEB (1977); MNB (1981); 9, WALA (1993). Years in parentheses are times of establishment of the stations.

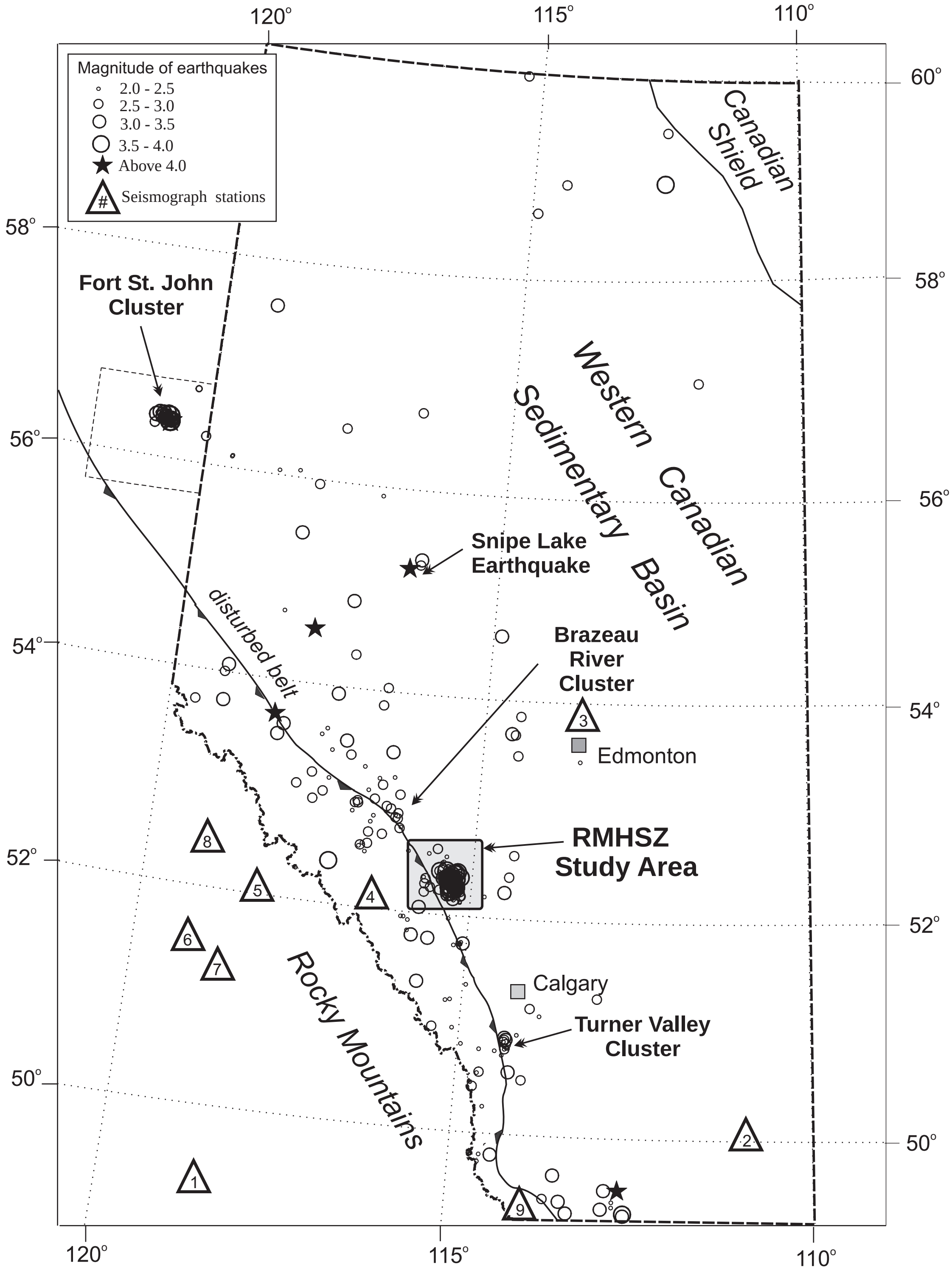

Some overpressuring is present at depth along the western edge of the basin, but most units are hydrostatically pressured, or underpressured. The only potential décollement zone, where geomechanical detachment might take place, is the Lower Devonian halite-rich section of the Prairie Evaporite. However, similar oriented horizontal stresses above and below this unit suggest that the entire sedimentary section is attached to the basement (Bell 1996). The stress regime is directionally homogeneous (Fig. 1) in that S_{Hmax}, the maximum horizontal stress, is regionally oriented northeast–southwest across most of the basin (Bell and Gough 1979; Adams and Bell 1991). There is persuasive ev-

Fig. 3. Number of events ($M > 2$) recorded yearly in Alberta.

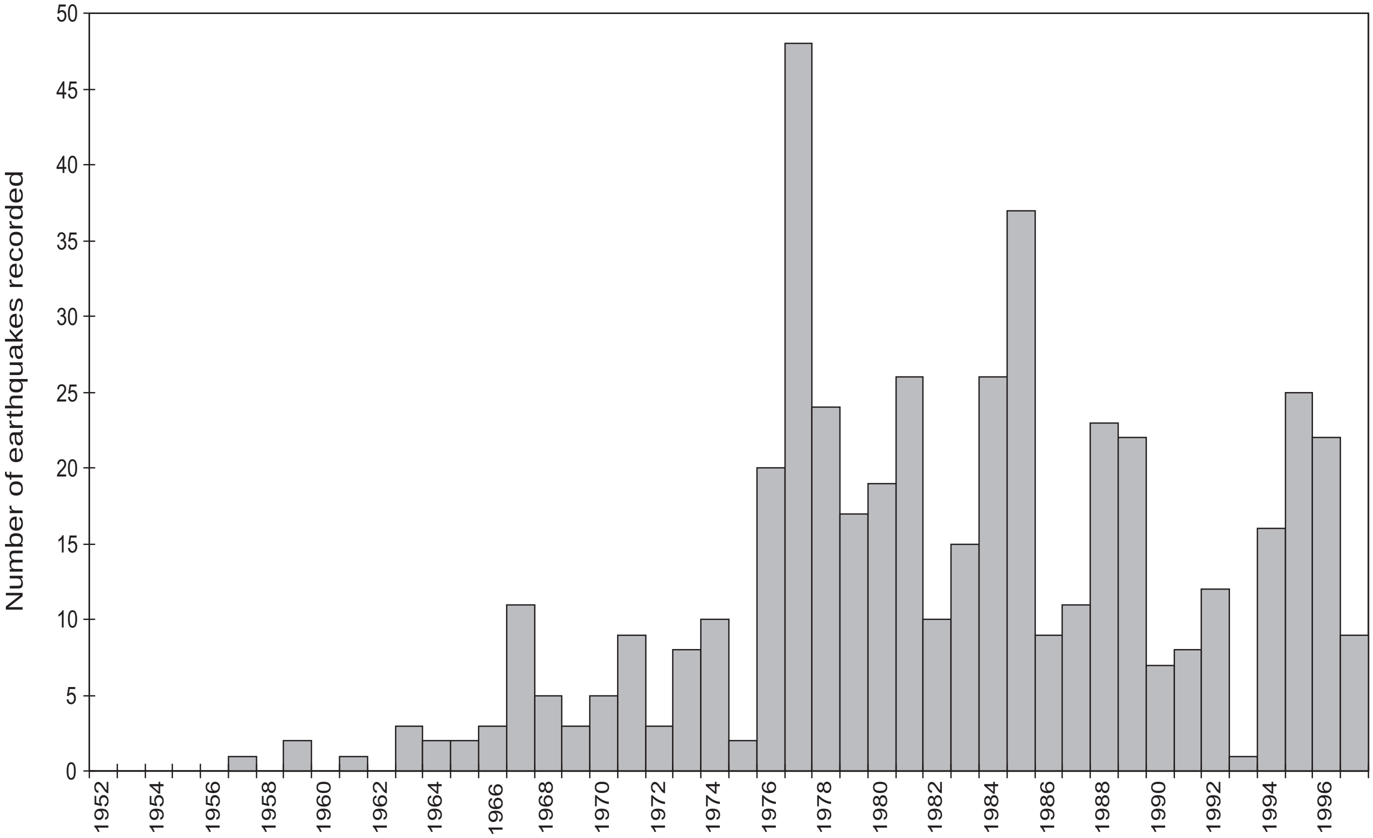

idence that horizontal stress magnitudes vary laterally within the Western Canada Sedimentary Basin. Bell (1996) presented a preliminary interpretation showing a systematic increase in the minimum horizontal stress (S_{Hmin}) gradients southwestwards towards the overthrust Rocky Mountain foothills, where S_{Hmin} magnitudes approach and locally exceed overburden stresses. The highest S_{Hmin} gradients so far documented come from foothill wells drilled in structural settings comparable to that of Rocky Mountain House. These elevated gradients may reflect paleostresses derived from the Laramide orogeny and (or) they may be an artifact of late Tertiary uplift and erosion. Thus, the differential stress $\sigma_1 - \sigma_3$ (where σ_1 and σ_3 are the largest and smallest principal stress, respectively) also increases toward the southwest (Fig. 1). This is important because it is the differential effective stress, together with the geomechanical properties of a rock unit, which determine its propensity to fracture. The basin is not highly active seismically (Rogers and Horner 1991). Earthquakes of magnitude 4 and greater are rare (Fig. 2). Most seismic events are barely felt and, except for a few earthquakes like the Snipe Lake event of March 1970 ($M = 5.1$), they have not caused alarm in this lightly populated region of Canada. The high seismicity of the intermontane belt that passes through Utah, Wyoming, and Montana south of the United States border (Smith and Arabasz 1991; Rogers and Horner 1991), does not extend northwards into the Western Canada Sedimentary Basin.

Available seismic data

The catalogue of earthquakes used in this study is a subset of the Canadian seismic events database for the last 100 years. The first recorded seismic event for the Alberta Basin occurred in 1957. Currently, there are four seismic stations located in Alberta, and the western Canadian earthquakes are recorded reliably by these stations together with many in British Columbia, Saskatchewan, Montana, and the Northwestern Territories. In Alberta, the catalogue lists 419 events with magnitudes up to 5.1. Events smaller than magnitude 2 were included only from 1993. Many more smaller events would be recognised if a denser seismometer grid was employed. Rebollar et al. (1984) recorded 220 events between January 1976 and February 1980 with magnitude less than 4 in the Rocky Mountain House area. This is twice the total number of events in the catalogue for the same period. The catalogue lists the time of a seismic event, its location, its magnitude, and the felt area. The depth has not been determined for most events. Rebollar et al. (1982, 1984) and Wetmiller (1986) attempted to determine the depth of specific earthquakes in the Rocky Mountain House Seismic Zone (RMHSZ), but the results are inconclusive.

General pattern of seismicity of the Alberta Basin

Figure 2 portrays earthquakes that occurred in Alberta prior to March 1996. Seismic events are more or less evenly distributed along the Alberta foreland fold and thrust belt (disturbed belt), except for major clusters at Turner Valley, Rocky Mountain House, and Brazeau River. Figure 3 shows the number of seismic events per year for this area. The increase in number of earthquakes in recent years cannot be explained fully by the improvement of the seismic network. Horner and Hasegawa (1978) discuss the spatial and temporal distribution of seismograph stations in western Canada.

Fig. 4. (*a*) Seismicity of RMHSZ. (*b*) Approximate location of the hydrocarbon fields of RMHSZ, showing all the producing wells and cross section A–A′.

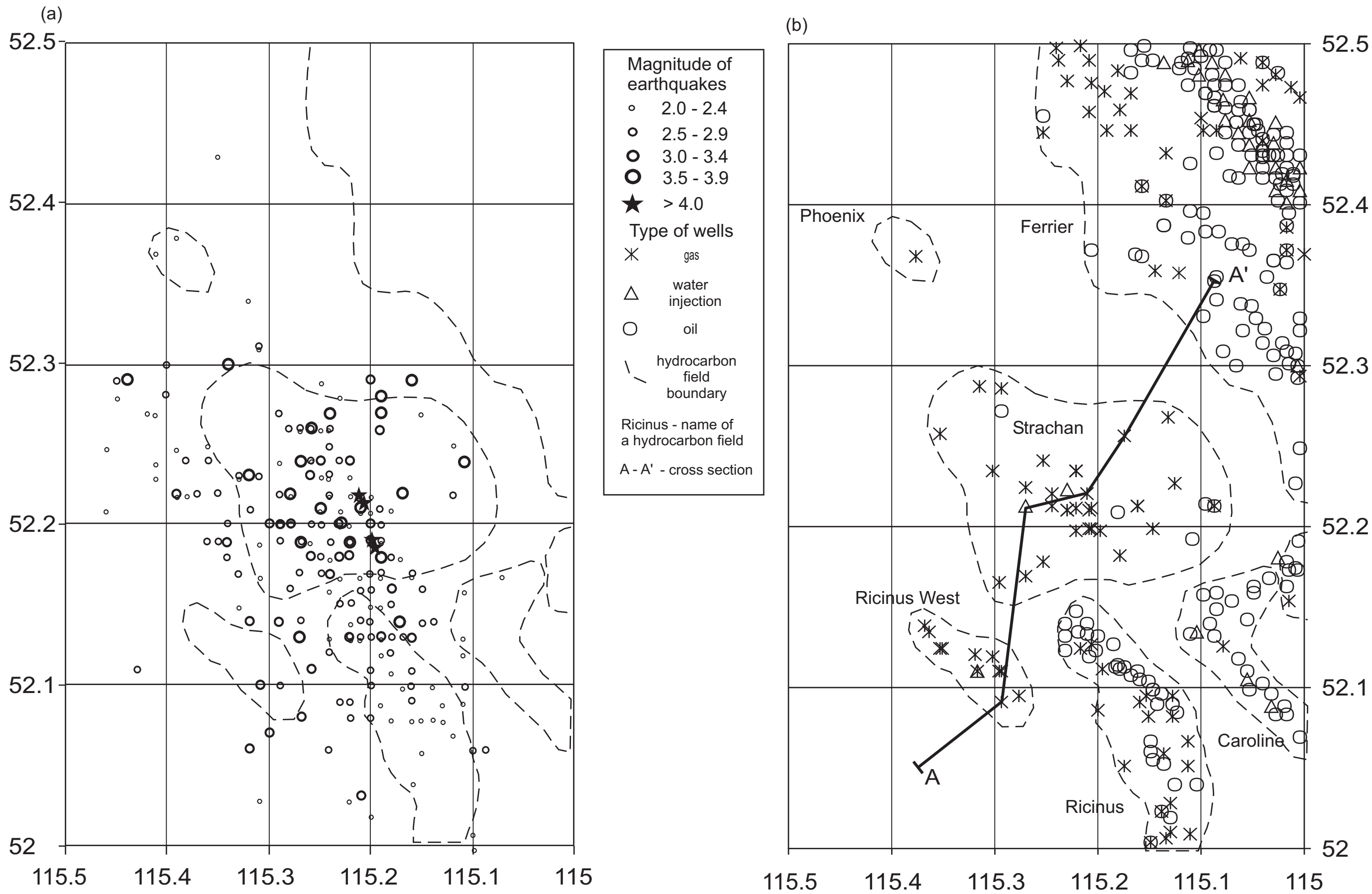

For the period 1936–1956 there was one seismic station in Alberta (in Banff), one in Saskatchewan, and one in Montana. By 1966, seismic events in the RMHSZ were being registered by more than six seismic stations in Alberta, British Columbia, Saskatchewan, and Montana.

We selected the RMHSZ cluster of events for closer investigation into the possible causes of the seismicity. This choice was made because this is the main area of concentrated seismicity in Alberta, it is the oldest producing zone which is also still active seismically, and it is the area with the largest amount of relevant data, including focal-mechanism solutions and gas production statistics. The study encompasses the region between 52° and 52°30′N and 115° and 115°30′W, and covers approximately 700 square miles. It includes Strachan, Phoenix, part of Ricinus, Ricinus West, the western part of Ferrier, and Caroline fields (Fig. 4).

Induced seismicity in the Rocky Mountain House area

Statistical analysis

Figure 4*a* shows the seismic events, and Fig. 4*b* portrays all the producing wells (oil, gas, and water injection) in the study area. The earthquakes are mostly concentrated within the Strachan field, which produces mainly gas (five oil wells out of 36 producing wells). No seismic events have been observed around the western part of the Ferrier field or around Caroline, both of which produce mainly oil. Ricinus produces half oil and half gas and is characterized by high seismic activity of variable magnitude in the vicinity both of the gas and oil producing wells. In addition, many seismic events were recorded around Ricinus West, which is mainly a gas-producing field. As can be seen, the seismic events in the study area are concentrated mainly in the vicinity of gas-producing pools and they are far less abundant near oil-producing areas.

As reported by Wetmiller (1986), Horner et al. (1994), and an in-house database of the Geological Survey of Canada (Calgary), high-pressure water injection has been carried out for only two wells at Strachan. Water injection was carried out at Ferrier, but there are no associated seismic events (Fig. 4).

The data on gas production are provided by the Alberta Energy and Utilities Board (1996) for the Strachan, Ricinus, and Ferrier fields. Figure 5 shows the high correlation coefficient (r = 0.61) between gas-production volumes and number of seismic events for Strachan D3-A gas pool from 1976 to 1995. There is a lag between the commencement of production (1970) and the onset of seismic events (1975–1976). The significance of this lag will be discussed later. Between 1976 and 1995 there is a strong correlation between the incidence of seismic events and fluctuations in production.

Figure 6 is a contour map of the depths of producing wells which also shows the location and magnitudes of seismic events. The majority of the seismic events are enclosed

Fig. 5. Relationship between gas production and seismicity for Strachan D3-A pool; $r = 0.61$ (1976–1995).

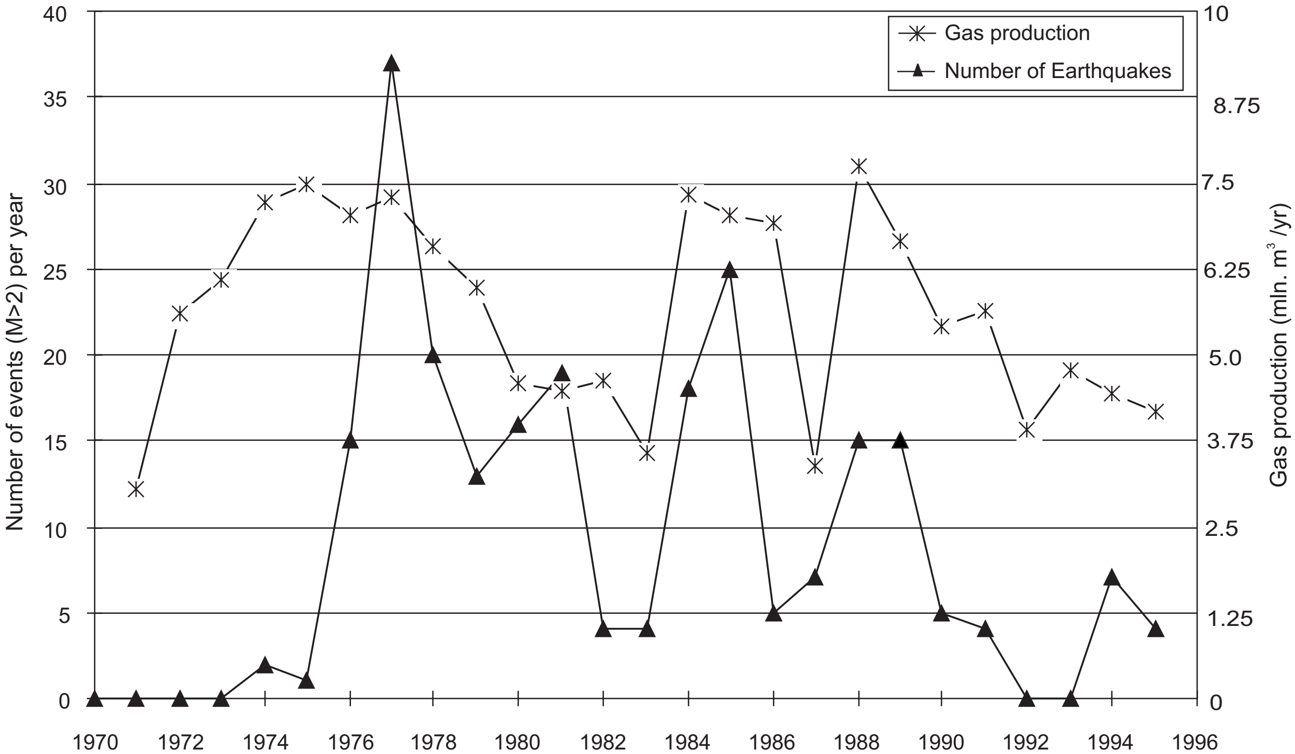

by the 3000 m contour. The Snipe Lake event (Milne 1970) is not shown on Fig. 6, but it also occurred in an area where the production wells were deeper than 2500 m. There are 646 oil and gas wells within 80 km of Snipe Lake with average depths of 2600 m. It appears that the wells shallower than 2500 m do not play an important role in generating induced seismicity in the Western Canada Sedimentary Basin. Similar well depth – seismicity relationships have been reported elsewhere. Beneath the Lacq gas field in southwest France, induced earthquake epicentres coincide areally with wells drilled deeper than 3200 m (Grasso 1992). In the Gazli and Grozny gas fields in the former Soviet Union which are famous for their devastating induced seismicity (Smirnova et al. 1975; Plotnikova et al. 1989), the majority of the events occurred in proximity to wells deeper than 3000 m.

In the study area, the seismic monitoring program run by Wetmiller in 1980 (Wetmiller 1986) demonstrated that the majority of the events were concentrated within a thin horizontal interval approximately 5000 m below the surface (4000 m below sea level) and at an average of 900 m below the Devonian Leduc carbonates from which gas has been extracted at Strachan, Ricinus, and Ricinus West (Fig. 7). Wetmiller (1986) deployed five Sprengnether MEQ-800 smoked-paper seismographs and one Sprengnether DR-100 three-component digital seismograph. Over a 3 week period, 14 sites were occupied. One hundred and forty six microearthquakes were recorded by the network, of which 67 were located. Epicentres were located in the basal Cambrian sequence and within the Precambrian basement.

Analytical approach

It is not intuitively obvious why gas production, unaccompanied by fluid injection, should trigger earthquakes. Nor does it seem reasonable that these earthquakes should occur beneath the rocks from which fluids were withdrawn. This conundrum has been resolved by Segall (1985), who employed Biot's Theory (Rice and Cleary 1976) to show how changes in fluid content within a reservoir can result in modifications to the stress regime in adjacent and underlying rocks and that, in specific circumstances, these changes can trigger seismicity. Segall's approach is followed in this study. Where possible, we have used measured quantities, but some parameters have had to be estimated, as discussed below. The material properties used in the calculations are listed in Table 1. The geometry of the field used is shown in Fig. 8. To simulate conditions that might trigger seismicity, we have simplified the geometry of the Strachan D-3A pool so as to analyse a linear accumulation. This is portrayed schematically in Fig. 8.

The rate of liquid extraction per year for gas is reported (Alberta Energy and Utilities Board 1996) without taking into account the gas formation volume factor. Slider (1976) derives the gas formation volume factor (B_g) as

$$[1] \qquad B_g = \frac{znRT}{5.615P}$$

where P is the pressure in psi (1 psi = 6.895 kPa), z is a deviation factor, n is the number of moles (1/379), R is Rhydberg's constant, and T is the temperature in K. With this relationship, a revised figure for gas extraction that gives the true volume of gas extracted from the reservoir pore spaces was obtained. Fluid compressibility for gas (β) is taken from Alberta Energy and Utilities Board (1996) for gas subject to a pressure of 7000 psi, the virgin reservoir pressure at Strachan (Rose 1990). The viscosity of gas (η) is taken from McCain (1973) and equated to the viscosity of

Fig. 6. Relationship between the seismicity and the depth of producing in RMHSZ.

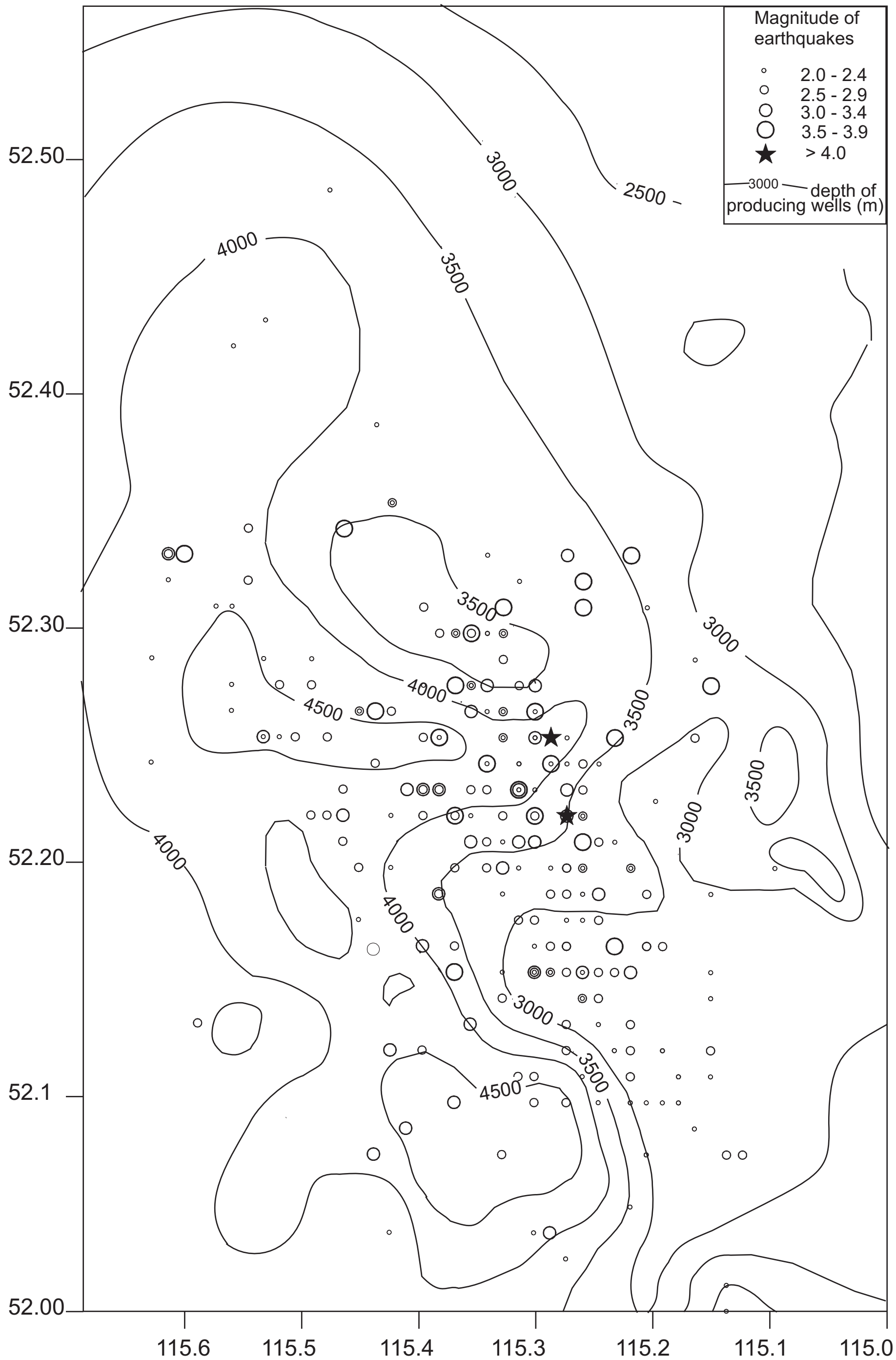

methane at 7000 psi and 124°C. Skempton's coefficient (B), Poisson's ratios (both drained ν and undrained ν_u), and the shear modulus (μ) are not reported for the Strachan field, or for any other fields in the Western Canada Sedimentary Basin. The values used are from Rice and Cleary (1976) as estimated for Tennessee marble. The density of limestone (ρ) is taken from Anderson et al. (1989) and conformed with density log measurements at the 10-31-37-9W5 well. The shear modulus μ is estimated using the equation

$$[2] \qquad \mu = \rho V_s^2$$

where the sheer wave velocity V_s = 3200 m/s, and density is known. V_s is derived from V_p/r, where the compressional wave velocity V_p = 5500 m/s as reported by Anderson et al. (1989), and the reflection coefficient r is derived from

$$[3] \qquad \nu_u = \frac{(r^2 - 2)}{2(r^2 - 1)} = 0.16$$

where ν_u is the undrained Poisson's ratio.

Diffusivity c is estimated after Segall (1985) as

Fig. 7. Cross section through the RMHSZ (A–A′ in Fig. 4). Approximate location of the earthquake swarm is after Wetmiller (1986). bmsl, below mean sea level.

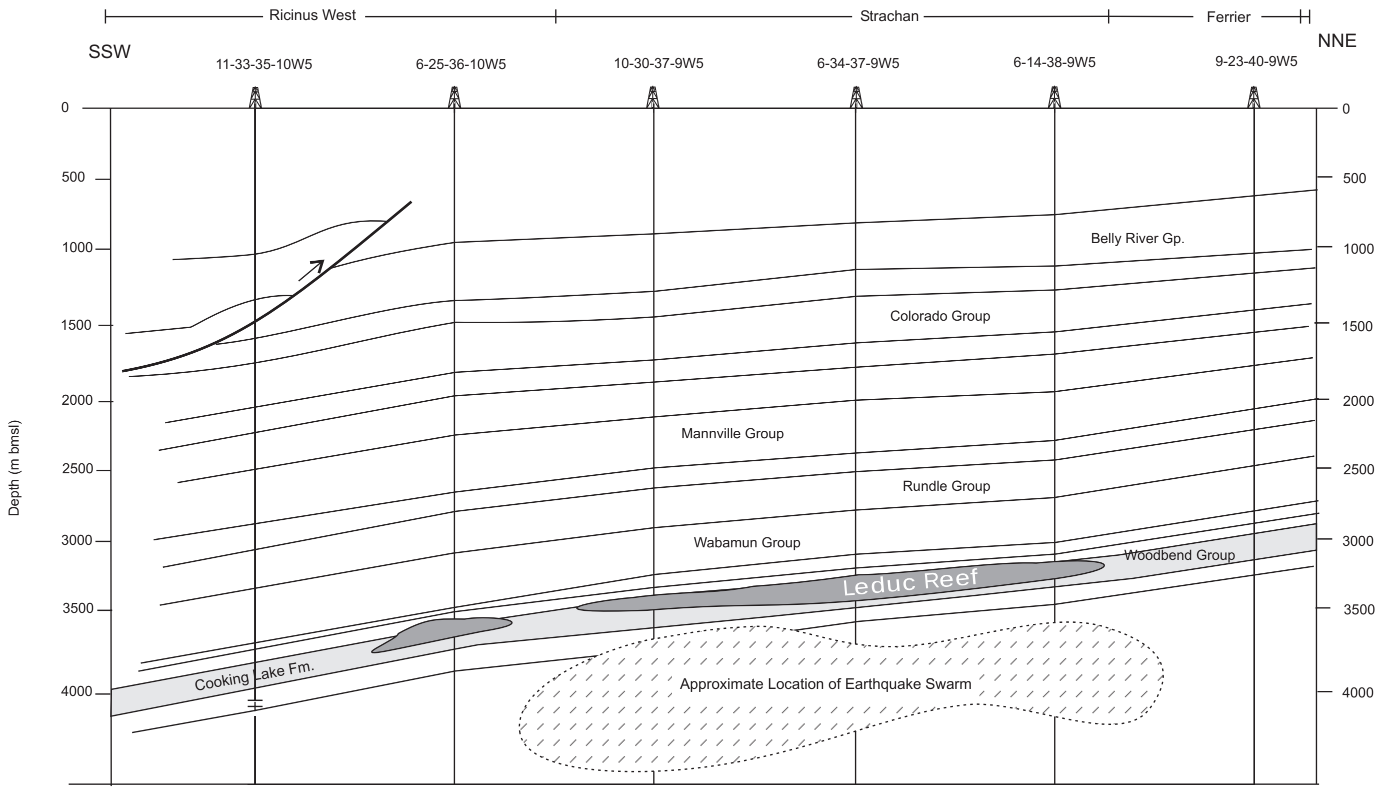

Table 1. Average properties of the producing horizon, Strachan D-3A pool.

Parameter	Symbol	Value	References
Depth (km)	D	4.100	Rose 1990
Thickness (m)	T	115 (net pay)	Alberta Energy and Utilities Board 1996
Average rate of gas extraction (m^3/year)	V	2.62×10^6	Alberta Energy and Utilities Board 1996
Extraction starts (year)	—	1971	Alberta Energy and Utilities Board 1996
Characteristic length along strike (km)	L	7	Rose 1990
Average porosity	ϕ	0.082	Alberta Energy and Utilities Board 1996
Permeability (m^2)	κ	2.46×10^{13}	Rose 1990
Fluid compressibility (Pa^{-1})	β	1.6×10^{-4}	Alberta Energy and Utilities Board 1996
Viscosity (Pa·s)	η	31×10^{-6}	McCain 1973
Diffusivity (m^2/s)	c	0.6×10^{-3} (1.89×10^4 m^2/year)	See text
Skempton's coefficient	B	0.51	Rice and Cleary 1976
Poisson's ratio (undrained)	ν_u	0.16	Carmichael 1984
Poisson's ratio (drained)	ν	0.14	Carmichael 1984
Density of limestone (kg/m^3)	ρ	2750	Carmichael 1984; Anderson et al.1989
Shear modulus (Pa)	μ	3.367×10^9	See text

[4] $$c = \frac{\kappa}{\eta\phi\beta}$$

where ϕ is the porosity, β is the fluid compressibility, η is the fluid viscosity, and κ is the permeability. The changes in pore-fluid content (M) are calculated as

[5] $$M(y, t) = -\frac{V}{LT\phi}(t / c)^{1/2}\,\mathrm{ierfc}\left(\frac{y^2}{4ct}\right)$$

where V is the extracted volume, L is the length along strike, T is the thickness, t is the duration in years, y is the distance from the point of extraction, and ierfc(x) is the first integral of the complementary error function and is given by the equation

[6] $$\mathrm{ierfc}(x) = \int_0^x \mathrm{erfc}(\xi)\mathrm{d}\xi = \frac{e^{-x^2}}{\sqrt{\pi}} - x[\mathrm{erfc}(x)]$$

where $x,y = \zeta, \xi$ at the point of extraction, where ζ and ξ are the vertical and horizontal coordinates.

Fig. 8. Permeable producing layer of thickness *T* buried at a depth *D* in a fluid-infiltrated, impermeable half-space. L, length of reservoir along strike.

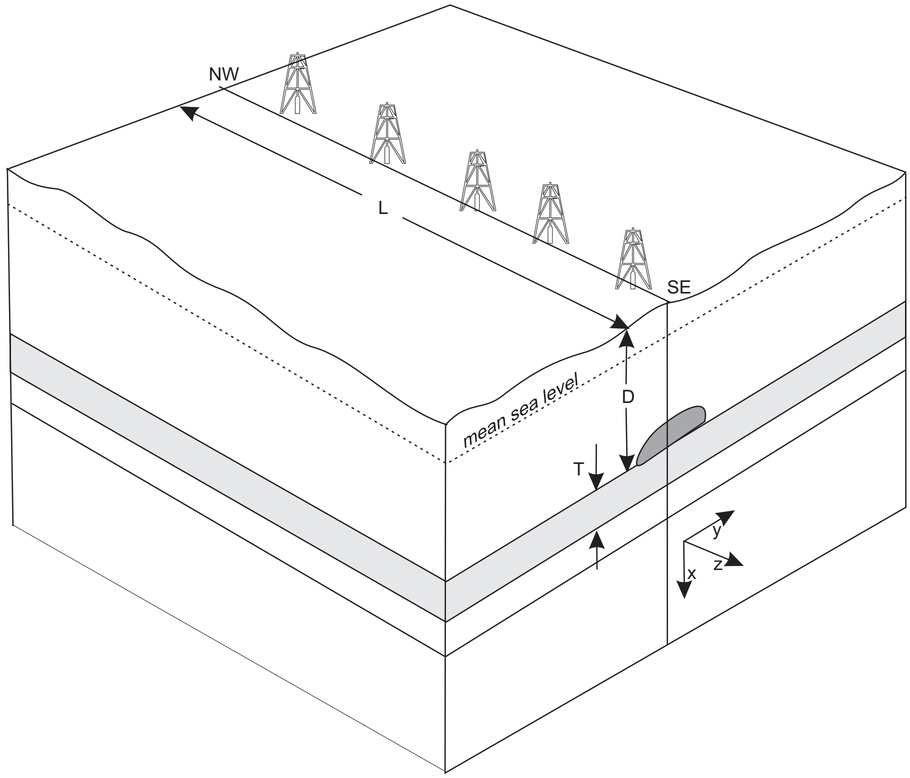

Fig. 9. Changes in pore-fluid content in fraction (variable rate of extraction for the Strachan field).

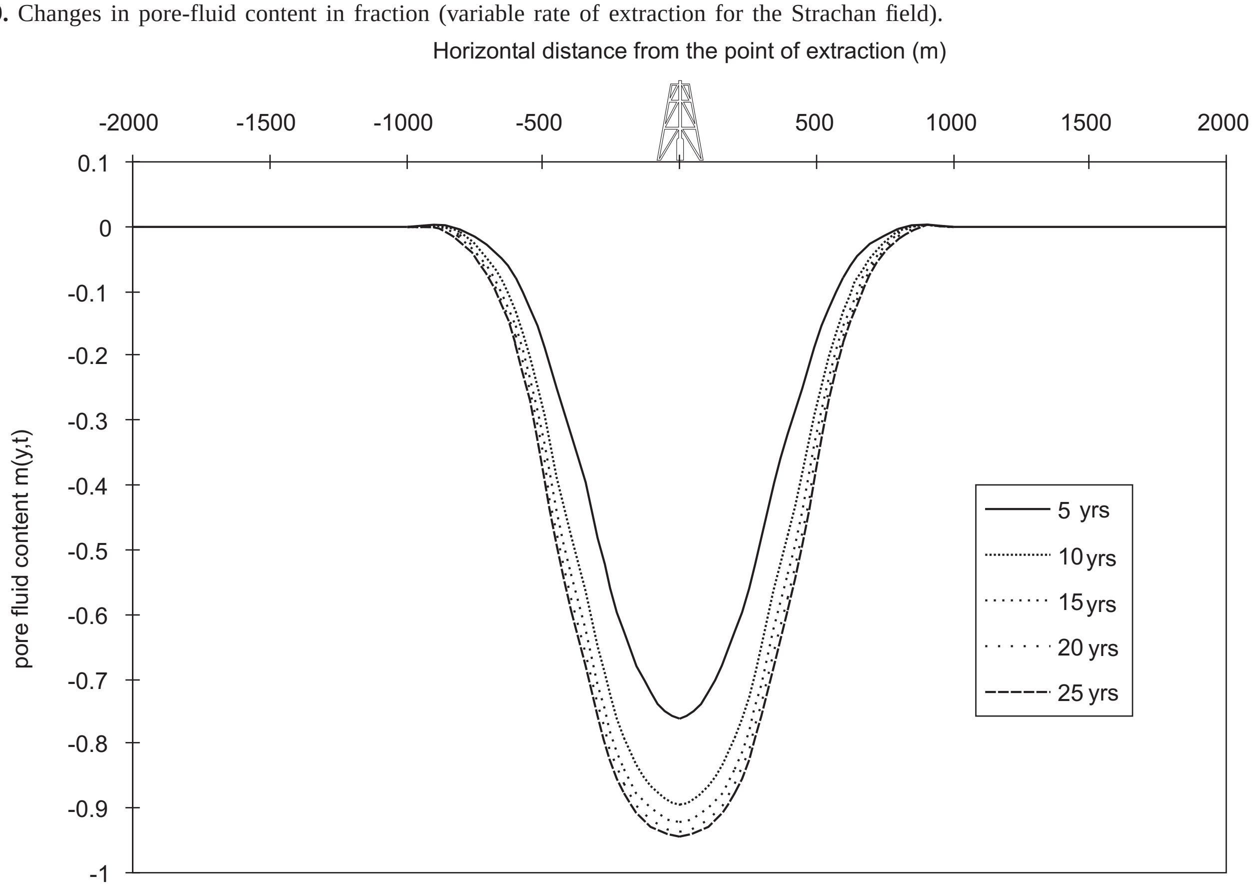

Table 2. Rate of production of Strachan field D-3A pool.

No. of years (n)	Production rate ($\times 10^3$ m^3/year) averaged from the onset of production	Production rate ($\times 10^3$ m^3/year) averaged for 5 years and used in the calculations
5	2744	2744 (1971–1976)
10	2337	1930 (1977–1982)
15	1893	1004 (1983–1988)
20	1580	640 (1989–1994)
25	1350	430 (1995–recent)

Fig. 10. Subsidence using variable rate of extraction in the Strachan field.

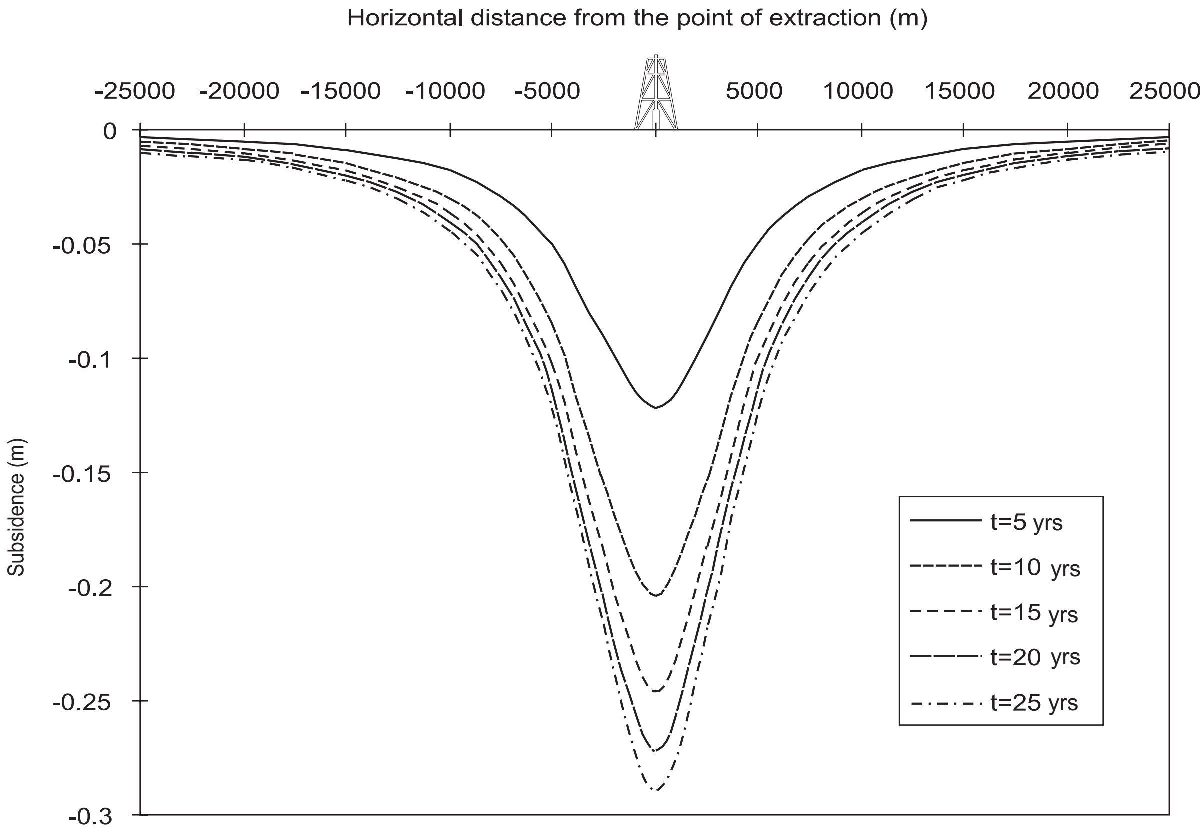

Subsidence u_x is calculated after Segall (1985) as

$$[7] \qquad u_x(x=0,y,t) = \frac{2B(1+\nu_u)\dot{V}D}{3\pi L}\left(\frac{t}{c}\right)^{1/2} \times \int_{-\infty}^{\infty} \frac{\mathrm{ierfc}(\xi^2/4ct)^{1/2}}{D^2+(y-\xi)^2}\mathrm{d}\xi$$

where D is the depth in metres, and $\dot{V}$ is the volume of gas extracted per year.

The following equations are used to calculate the stress changes σ_{mn} below the Strachan field:

$$[8] \qquad \sigma_{mn}(x,y,t) = \frac{-\mu B(1+\nu_u)\dot{V}}{3\pi(1-\nu_u)L}\left(\frac{t}{c}\right)^{1/2} \times \int_{-\infty}^{\infty} G_{mn}(x,y,D,\xi)\,\mathrm{ierfc}\left(\frac{\xi^2}{4ct}\right)^{1/2}\mathrm{d}\xi$$

where m, n = x, y, and the Green functions G_{mn} are

$$[9] \qquad G_{xx} = \frac{(y-\xi)^2-(x-\zeta)^2}{r_1^4} + \frac{(5x+\xi)(x+\zeta)-(y-\xi)^2}{r_2^4} - \frac{16x(x+\zeta)(y-\xi)^2}{r_2^6}$$

$$[10] \qquad G_{yy} = \frac{(x-\zeta)^2-(y-\xi)^2}{r_1^4} + \frac{(x+\zeta)(3\zeta-x)-3(y-\xi)^2}{r_2^4} - \frac{16x(x+\zeta)(y-\xi)^2}{r_2^6}$$

Fig. 11. Incremental changes in magnitude of vertical stress field (MPa) below Strachan reservoir (D3-A pool) shown on a southwest–northeast vertical plane, after 5 years (solid lines) and 20 years (broken lines) of gas extraction. ★, approximate location of the seismic event.

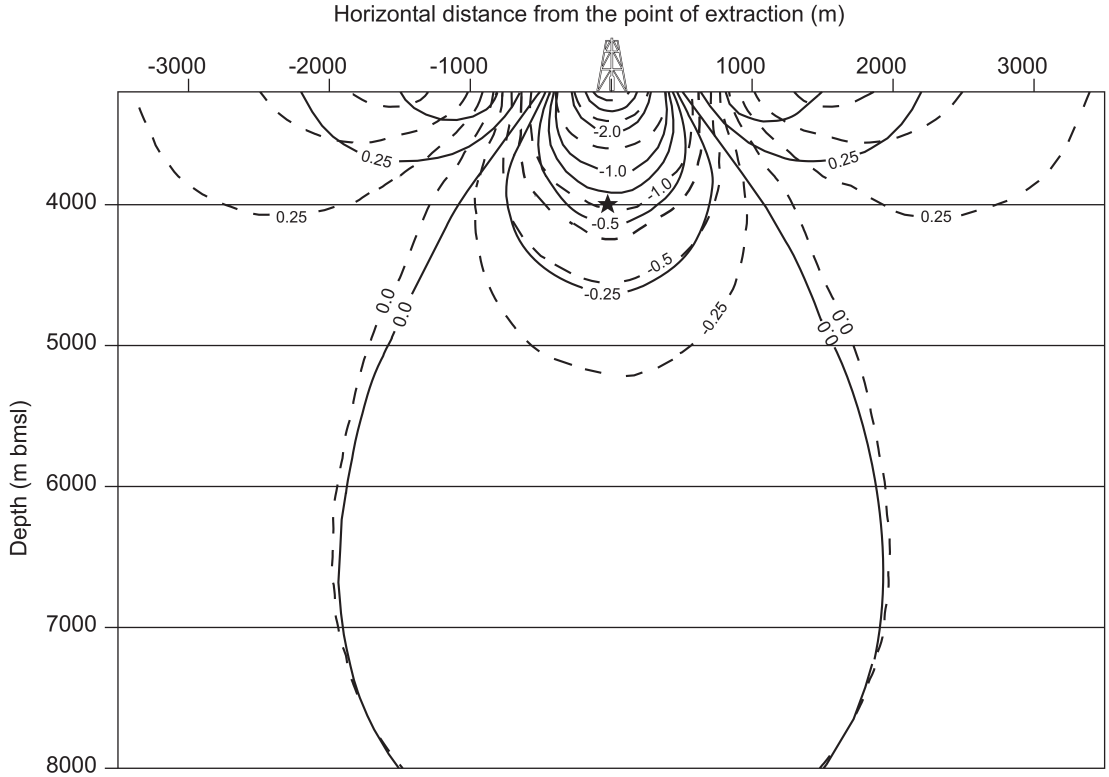

Fig. 12. Incremental changes in magnitude of horizontal stress field (MPa) below Strachan reservoir (D3-A pool) shown on a southwest–northeast vertical plane, after 5 years (solid lines) and 20 years (broken lines) of gas extraction. ★, approximate location of the seismic event.

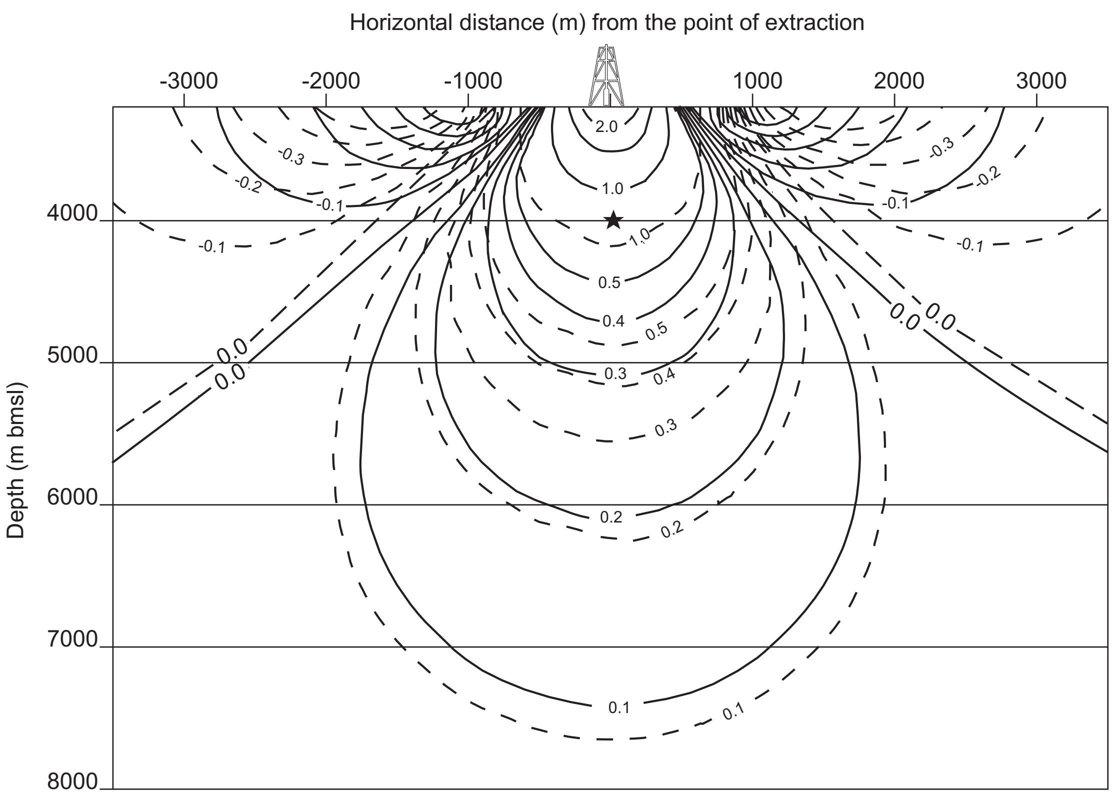

Fig. 13. Incremental changes in magnitude of mean stress field (MPa) below Strachan reservoir (D3-A pool) shown on a southwest–northeast vertical plane, after 5 years (solid lines) and 20 years (broken lines) of gas extraction. ★, approximate location of the seismic event.

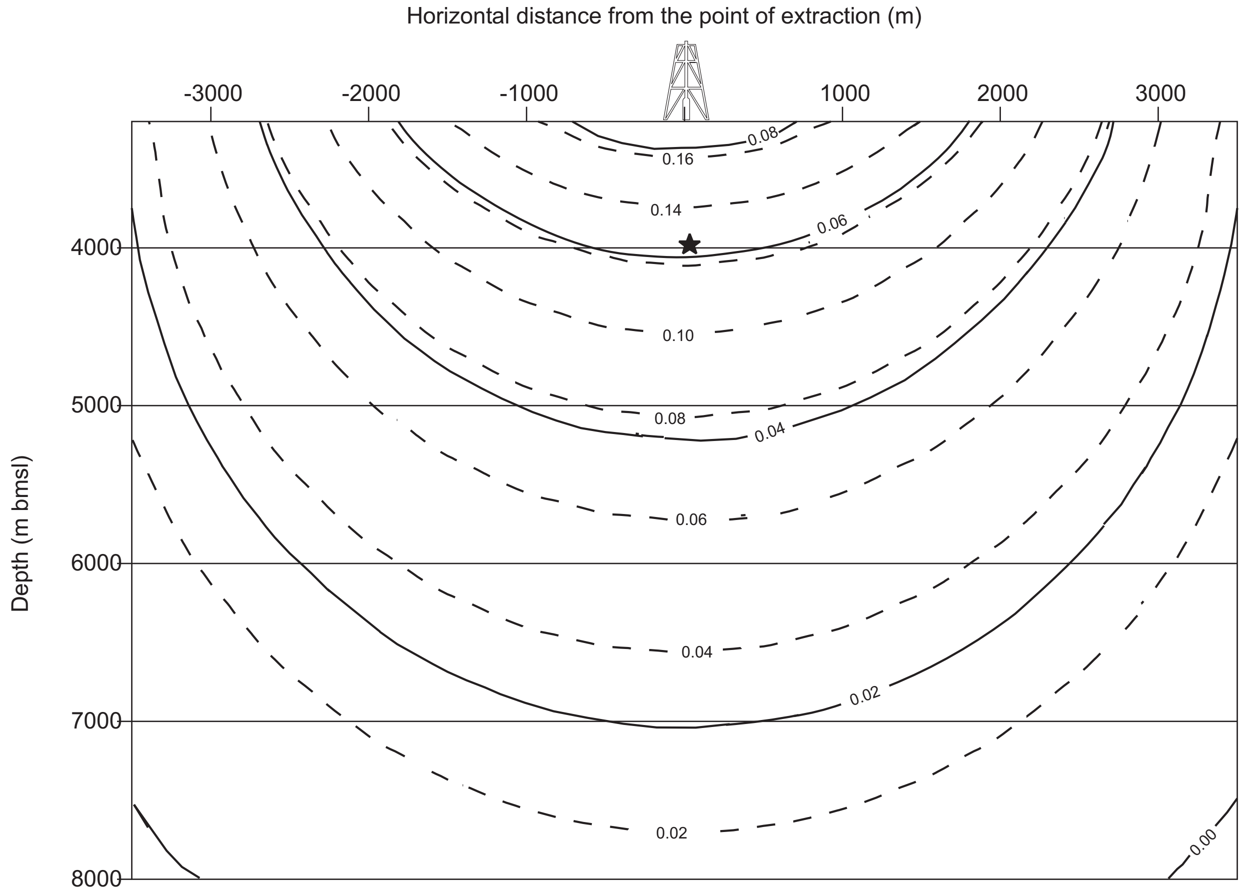

$$G_{xy} = \frac{-2(y-\xi)(x-\zeta)}{r_1^4} - \frac{2(y-\xi)(3x+\zeta)}{r_2^4} - \frac{16x(x+\zeta)^2(y-\xi)}{r_2^6} \quad [11]$$

where $r_1^2 = (x-\zeta)^2 + (y-\xi)^2$ and $r_2^2 = (x+\zeta)^2 + (y-\zeta)^2$.

Pore-fluid content changes and subsidence due to gas production

Figure 9 shows the changes in pore-fluid content calculated from eq. [5]. The rate of extraction is used averaged for each 5 year increment of production (Table 2):

$$M_{\text{total}} = M_{n-5} + (1 - M_{n-5})M_n \quad [12]$$

where M_{total} is the net change of pore-fluid content after n years of production. Figure 9 shows that nearly 70% of fluid content was extracted for the first 5 years of production. Fluid extraction will be associated with reservoir compaction and surficial subsidence above the reservoir.

The above theory is also used to calculate the subsidence which might have occurred above the Strachan field as a result of gas extraction. Unfortunately, we are unable to relate the calculated results to observations due to lack of data. The most recent map of vertical crustal movements compiled by the Geological Survey of Canada (Vanicek and Nagy 1980) shows negligible movements close to 0 cm/year in the vicinity of RMHSZ due to lack of resolution.

The parameters used in the calculation are the same as those used previously. It is clear that the subsidence increases linearly with the rate of fluid extraction and depends on hydraulic diffusivity. Figure 10 shows the calculated rate of subsidence due to variable rate of extraction (for 5, 10, 15, 20, and 25 years). For the first 5 years of gas production, when the rate of extraction was the highest (see Table 2), the subsidence could reach 25 mm/year, decreasing to 11 mm/year after 25 years of gas production. As mentioned above, we cannot compare calculated results with observed ones. However, it is worth noting that Segall's (1985) calculated results coincide well with the observed ones and give 3–6 mm/year due to oil extraction. According to Maury et al. (1992), the average rate of subsidence of the Lacq gas field in France for 20 years of extraction is 2.1 mm/year, although the production rate is much lower than that at Strachan.

Changes of stress fields below Strachan field because of production

Changes in vertical (σ_{xx}) and horizontal (σ_{yy}) stresses below the Strachan D-3A pool are calculated according to eq. [8]. The parameters used for the calculations are given in Table 1. The changes in stresses are plotted in the x–y plane which is perpendicular to the strike of the pool and is ap-

Fig. 14. Incremental changes in magnitude of deviatoric stress field (MPa) below Strachan reservoir (D3-A pool) shown on a southwest–northeast vertical plane, after 5 years (solid lines) and 20 years (broken lines) of gas extraction. ★, approximate location of the seismic event.

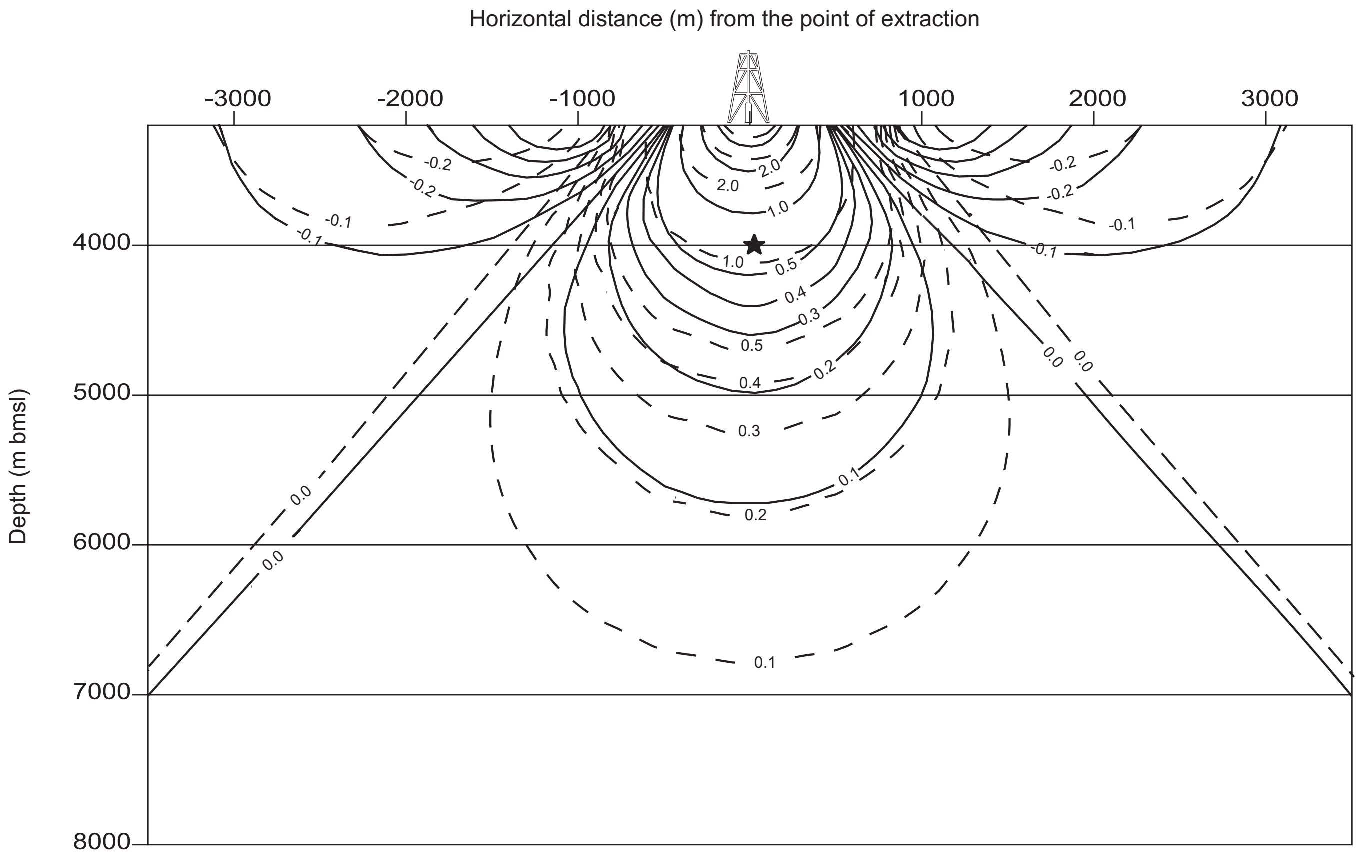

proximately parallel to the direction of the S_{Hmax} (Figs. 11, 12). Calculations were made for 5 and 20 years after extraction started in 1971. In this paper the positive stresses are always treated as compressions.

The mean stress [$(\sigma_{xx} + \sigma_{yy})/2$] (Fig. 13) and the deviatoric stress changes [$(\sigma_{xx} - \sigma_{yy})/2$] (Fig. 14) are plotted on the same *x*–*y* plane. It is notable that the changes in mean stress are very small (0.1 MPa) as compared with the deviatoric stresses, which are of the order of 1 MPa. This phenomenon can be explained by the fact that due to extraction the changes in vertical stress are negative (dilatation), whereas the changes in horizontal stress (see Fig. 12) are positive (compression).

The above stress changes are then applied to the focal-mechanism solution of the 3.9 magnitude RMHSZ earthquake that occurred on 19 October 1996 (R. Horner, personal communication, 1997). This yielded two solutions, NP1 302/51° northeast and NP2 156/44° southwest, at an approximate depth of 4 km below sea level (Fig. 15), which is 1 km below the Strachan D3-A pool.

It is interesting to note that the strike of the D3-A pool is almost the same as the strike of the fault planes suggested by the focal-mechanism solution (northwest–southeast 302 and 336). The vertical and horizontal stresses are resolved into normal, shear, and driving stresses on the two planes and are plotted in Figs. 16 and 17. These stresses represent the changes of magnitude in the existing stress state due to gas production from the Strachan D3-A pool.

Fig. 15. Lower hemisphere equal area projection of the best fitting double-couple solution of the focus for a seismic event (M = 3.9), dated 19 October 1996 at Rocky Mountain House, Alberta (52°13′N, 115°13′W), which occurred at an estimated depth of 4.0 km below mean sea level (R.B. Horner, personal communication, 1997).

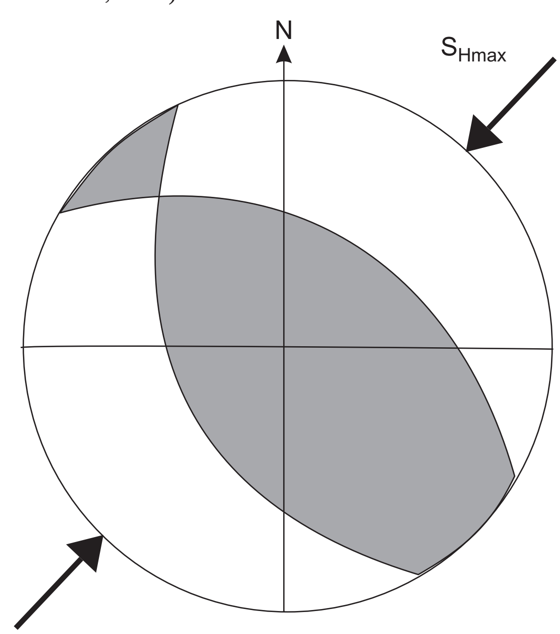

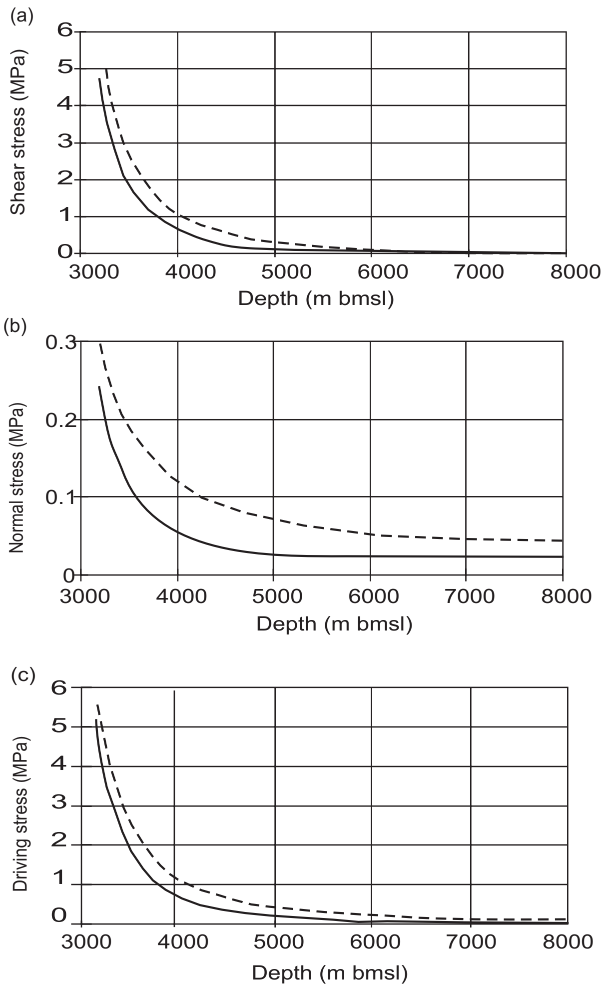

Fig. 16. Incremental changes in magnitude of shear (*a*), normal (*b*), and driving (*c*) stresses with depth at a plane dipping 44° southwest below the Strachan field after 5 years (solid lines) and 20 years (broken lines) of gas production.

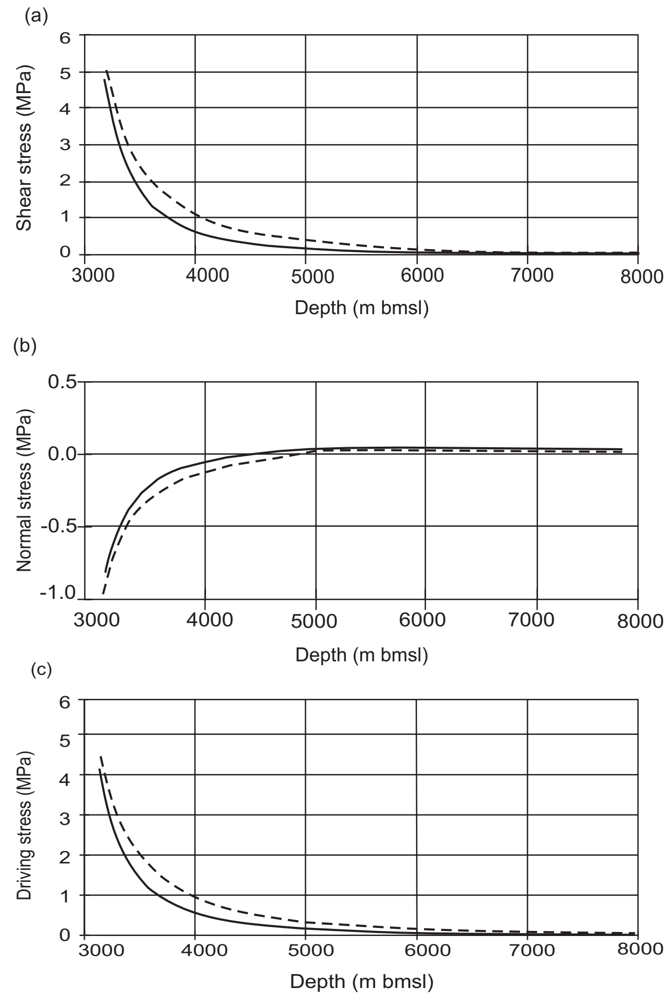

Fig. 17. Incremental changes in magnitude of shear (*a*), normal (*b*), and driving (*c*) stresses with depth at a plane dipping 51° northeast below the Strachan field after 5 years (solid lines) and 20 years (broken lines) of gas production.

The change in driving stress ($\Delta\sigma_d$) acting to cause displacement is calculated following Segall (1985) as

[13] $$\Delta\sigma_d = \Delta\sigma_s + f(\Delta\sigma_n + \Delta p)$$

where $\Delta\sigma_s$ and $\Delta\sigma_n$ are the changes in shear and normal stresses, respectively; f is the coefficient of friction; and Δp is the change in pore pressure. Change in pore pressure is calculated as

[14] $$\Delta p = \frac{(1 + \nu_u B)}{3}\Delta\sigma_{nn}$$

where $\Delta\sigma_{nn}$ is the change in mean stress.

The positive sign of shear stress on both planes favours reverse faulting up to 8 km below the Strachan field (Figs. 16*a*, 17*a*). Note that the changes in the magnitudes of shear stress are quite high; it decreases from 4.5 MPa right below the reservoir to approximately 1 MPa at 4 km below sea level, the depth of the seismic event. Changes in magnitude of normal stress at both planes are relatively low, as shown in Figs. 16*b* and 17*b*. On the southwest-dipping plane it represents compression, whereas on northeast-dipping plane it represents dilatation. The changes in magnitudes of normal stress on both planes decrease with depth.

The changes in driving stress on the southwest- and northeast-dipping planes are shown in Figs. 16*c* and 17*c*, respectively. Changes in driving stresses after 5 and 20 years of gas production favour reverse faulting and show the sharp decrease in magnitudes from 4 MPa right below the reservoir up to almost nothing at a depth of 6 km.

Figure 18 depicts the inferred Mohr–Coulomb circle and failure line before and after the gas extraction. Since we do not know the exact value of the coefficient of friction for the rocks in which failure occurred, the most common value (0.6) is used. Figure 19 shows changes of S_{Hmin} with depth based on hydraulic fractures run in Mesozoic rocks in the Caroline, Ricinus, and Strachan fields (McLellan 1989). A value of 120 MPa was assigned for S_{Hmin} at the depth of earthquake occurrence (4000 m below mean sea level). Note that a change of only 1 MPa in stress is apparently sufficient to produce the failure under the recent rate of extraction (Fig. 18). The proposed mechanism of failure suggests that the overburden pressure (vertical stress) is decreasing while

Fig. 18. Schematic representation of the Mohr–Coulomb failure criterion applied to the stress regime in the Strachan area before extraction (circles formed using solid lines) and after extraction (circles formed using broken lines). The significance of this simulation is explained in the text. S_{Hmax}', maximun horizontal effective stress; S_v and S_v', vertical stress and effective vertical stress, respectively; τ, sheer stress.

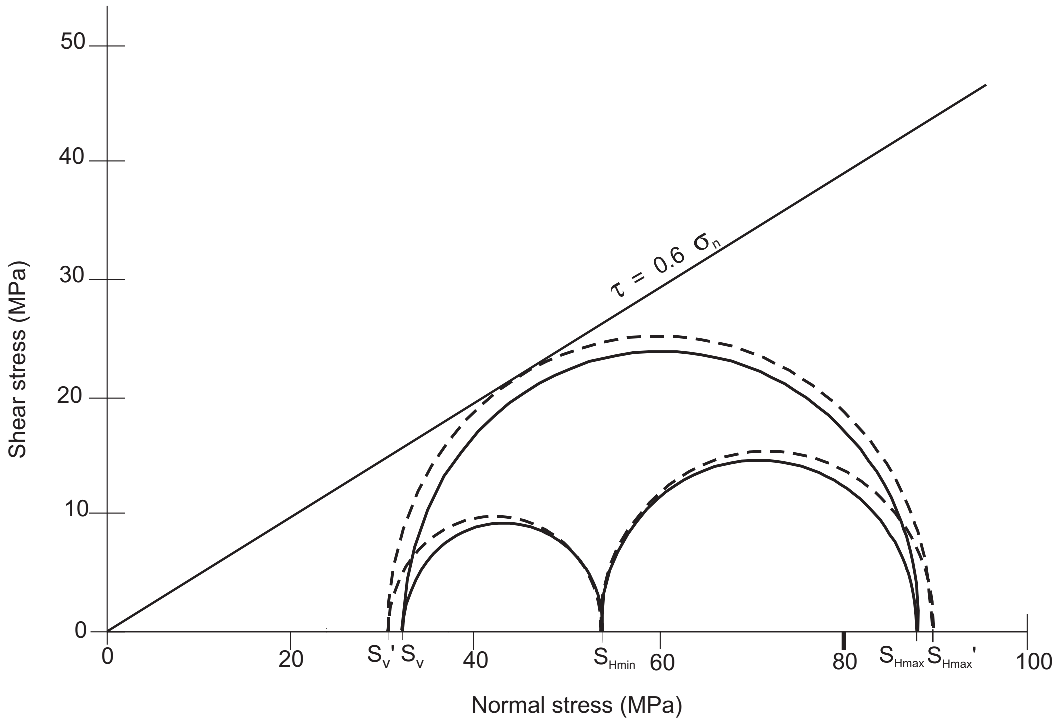

the normal stress is increasing due to extraction. This can explain the modest changes in mean stress which have the effect of increasing the radius of the Mohr's circle until it crosses the failure threshold. Since the stress regime and focal mechanism favour thrust faulting, we assume that failure occurred within a preexisting low-angle fault zone.

Discussion

The regional state of stress in the RMHSZ is close to the condition at which earthquakes could occur (Bell 1996), so small stress and strain changes could trigger seismic instabilities. We have shown that the rate of extraction (especially during the first 5 years for the Strachan field) can give rise to changes of stress magnitudes great enough to trigger earthquakes on reactivated faults. In the case of RMHSZ, the proximity to the disturbed belt and the instability of the state of stress are two factors that play important roles in generating the seismicity in the area.

There is no correlation between water injection and occurrence of earthquakes in the study area, although there are examples of seismic events caused by water injection in western Canada. According to Horner et al. (1994), earthquakes in the Fort St. John oil production area have been caused by massive water injection and occurred immediately after commencement of injection. We suspect that seismic events in Snipe lake, as well as in Turner Valley, were also caused by water injection. Water injection in the study area was carried out in several wells in the Ferrier, Ricinus West, and Strachan fields. The lack of seismic events associated with it allows us to conclude that the volume of water injected simply was not enough to cause stress release.

It is interesting to note that, in the case of Strachan (this paper), Lacq (Grasso and Wittlinger 1990), Gazli (Smirnova et al. 1975), and Grozny (Plotnikova et al. 1989) gas production areas, the onset of earthquake activity is very similar and started 5–10 years after gas extraction began. We believe that this period was required to accumulate the stresses needed to initiate movements on the faults in a "disturbed zone" (in our case) below the reservoir. Once the faults are activated, the failure line in Mohr–Coulomb criteria comes closer to the circle because of lowering of the coefficient of friction of the faults. So, it can explain the lack of correlation between the rate of production and seismicity of the Strachan field during the 5–7 years of extraction. However, the correlation increases dramatically after fault movements begin to occur below the reservoir.

There is no similarity in the relative depths of seismic events in the different gas production areas. At Strachan, reported seismic events occurred beneath the reservoir (Wetmiller 1986). However, most seismic events at Lacq occur above or within the reservoir (Grasso and Wittlinger 1990).

Conclusions

There are several observations which strongly suggest that the earthquakes that occurred in and around the Strachan field were triggered by gas extraction.

(1) These seismic events occurred in an area of naturally low seismicity, but high tectonic stresses.

Fig. 19. Approximate pore-pressure, S_{Hmin}, and S_v gradients estimated from the hydraulic fractures in the Caroline, Ricinus, and Strachan fields.

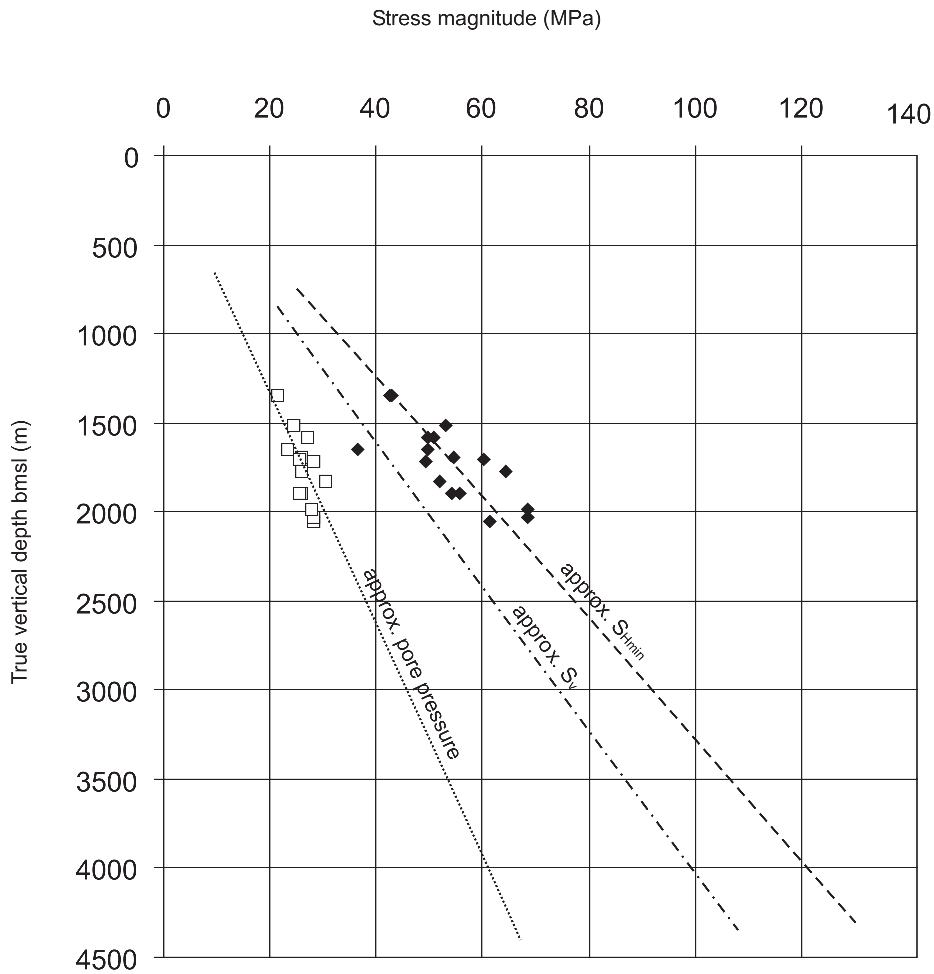

(2) There is spatial and temporal correlation between earthquake occurrence and the rate of gas production.

(3) There is no apparent correlation noted between extraction of oil and the number of seismic events. We speculate that the difference in density between gas and oil can account for this.

(4) There is no relationship between water injection and earthquakes for the study area.

(5) There is a linear correlation between depth of production and the number of seismic events.

(6) Application of the model developed by Segall (1985) shows that the 19 October 1996 earthquake below the D3-A pool of the Strachan field could have been triggered by gas extraction, which also would have caused subsidence and stress changes.

(7) Changes of stress due to extraction indicate a regime that favours reverse faulting and coincides well with the natural state of stress for this area. The proposed mechanism suggests decreasing pore pressure (vertical stress) and increasing normal stress so that changes of mean stresses are small and failure on preexisting faults can be initiated by increasing deviatoric stresses.

(8) As a consequence of the above, the high rate and long history of gas extraction can be considered as probable causes of triggering of the recent seismicity beneath the Strachan field.

Acknowledgments

This research was supported by the Geological Survey of Canada, Calgary. We thank R.B. Horner for his helpful comments and suggestions, and for providing the focal-mechanism solution and seismic events database. We are most grateful for the helpful comments and suggestions of the reviewers, Drs. J. Roest and G. Atkinson.

References

Adams, J., and Bell, J.S. 1991. Crustal stresses in Canada. *In* Neotectonics of North America. *Edited by* D.B. Slemmons, E.R. Engdahl, M.D. Zoback, and D.D. Blackwell. Geological Society of America, The Geology of North America, Decade Map Volume 1, pp. 367–385.

Alberta Energy and Utilities Board. 1996. Alberta reserves of crude oil, oil sands, gas, natural gas: statistics 1965–1996. Alberta Energy and Utilities Board, Calgary, Alta.

Anderson, N.L., Brown, R.J., and Hinds, R.C. 1989. Low- and high-relief Leduc formation reefs: a seismic analysis. Geophysics, **54**: 1410–1419.

Bell, J.S. 1996. In situ stresses in sedimentary rocks (part 2): applications of stress measurements. Geoscience Canada, **23**: 135–153.

Bell, J.S., and Gough, G.I. 1979. Northeast–southwest compressive stress in Alberta: evidence from oil wells. Earth and Planetary Science Letters, **45**: 475–482.

Bell, M.L., and Nur, A. 1978. Strength changes due to reservoir-induced pore pressure and stresses and application to Lake Oroville. Journal of Geophysical Research, **B9**: 4469–4483.

Carmichael, R.S. (*Editor*). 1984. Handbook of physical properties of rocks. Vols. I–III. CRC Press, Boca Raton, Fla.

Console, R., and Nikolaev, A. (*Editors*). 1995. Earthquakes induced by underground nuclear explosions. NATO ASI Series, Partnership Sub-Series 2. Environment, 4.

Davis, D.S., and Frohlich, C. 1993. Did (or will) fluid injection cause earthquakes? — criteria for a rational assessment. Seismological Research Letters, **64**: 207–224.

Davis, S.D., Nyffenegger, P.A., and Frohlich, C. 1995. The 9 April 1993 earthquake in South-Central Texas: was it induced by fluid withdrawal? Bulletin of the Seismological Society of America, **85**: 1888–1895.

Gendzwill, D.J., Horner, R.B., and Hasegawa, H.S. 1982. Induced earthquakes at a potash mine near Saskatoon, Canada. Canadian Journal of Earth Sciences, **19**: 466–475.

Gough, D.I. 1970. Load-induced earthquakes at Lake Kariba — II. Geophysical Journal of the Royal Astronomical Society, **21**: 79–101.

Gough, D.I. 1978. Induced seismicity. *In* Assessment and mitigation of earthquake risk. Proceedings of intergovernmental conference on the assessment of earthquake risk. UNESCO, Paris, pp. 91–117.

Grasso, J.R. 1992. Mechanics of seismic instabilities induced by the recovery of hydrocarbons. Pure and Applied Geophysics, **139**: 507–534.

Grasso, J.R., and Wittlinger, G. 1990. Ten years of seismic monitoring over a gas field. Bulletin of the Seismological Society of America, **80**: 450–473.

Gupta, H., and Rastogi, B. 1979. Dams and earthquakes. MIR, Moscow. (In Russian.)

Healy, J.H., Rubey, W.W., Griggs, D.T., and Raleigh, C.B. 1968. The Denver earthquakes. Science (Washington, D.C.), **161**: 1301–1310.

Horner, R.B., and Hasegawa, H.S. 1978. The seismotectonics of southern Saskatchewan. Canadian Journal of Earth Sciences, **15**: 1341–1355.

Horner, R.B., Barclay, J.E., and MacRae, J.M. 1994. Earthquakes and hydrocarbon production in the Fort St. John area of northeastern British Columbis. Canadian Journal of Exploration Geophysics, **30**: 39–50.

Hsien, P.A., and Bredehoeft, J.D. 1981. A reservoir analysis of the Denver earthquake: a case of induced seismicity. Journal of Geophysical Research, **86**(B2): 903–920.

Kisslinger, C. 1976. A review of theories of mechanisms of induced seismicity. Engineering Geology, **10**: 85–98.

Knoll, P. (*Editor*). 1992. Induced seismicity. A.A. Balkema Publishers, Old Post Road, Brookfield, Vt.

Leckie, D.A., Smith, D.G. 1992. Regional setting, evolution, and depositional cycles of the Western Canada Foreland Basin. *In* Foreland basins and fold belts. American Association of Petroleum Geologists (AAPG), Memoir 55, Chapt. 1, pp. 9–46.

Maury, V.M.R., Grasso, J.R., and Wittlinger, G. 1992. Monitoring of subsidence and induced seismicity in the Lacq gas field (France): the consequences on gas production and field operation. Engineering Geology, **32**: 123–135.

McCain, W.D., Jr. 1973. The properties of petroleum fluids. Petroleum Publication Co., Tulsa, Okla.

McGarr, A., Spottiswoode, S.M., and Gay, N.C. 1975. Relationship of mine tremors to induced stresses and to rock properties in the focal region. Bulletin of the Seismological Society of America, **65**: 981–993.

McLellan, P.J. 1989. In-situ stress magnitudes from hydraulic fracturing treatment records: a feasibility study. Geological Survey of Canada, Open File 1947.

Milne, W.G. 1970. The Snipe Lake, Alberta, earthquake of March 8, 1970. Canadian Journal of Earth Sciences, **6**: 1564–1567.

Milne, W.G., and Berry, M.J. 1976. Induced seismicity in Canada. Engineering Geology, **10**: 219–226.

Mossop, G., and Shetsen, I. (*Compilers*). 1994. Geological atlas of the Western Canada Sedimentary Basin. Canadian Society of Petroleum Geologists and Alberta Research Council, Edmonton, Alta.

Plotnikova, L.M., Flynova, M.G., and Machmudova, V.I. 1989. Induced seismicity in gas field region. *In* Proceedings of the 15th International Association of Seismology and Physics of the Earth Interior General Assembly, Istanbul, August 1989, pp. 31–32.

Pomeroy, P.W., Simpson, D.W., and Sbar, M.L. 1976. Earthquakes triggered by surface quarrying — the Wappinger Falls, New York, sequence of June 1974. Bulletin of the Seismological Society of America, **66**: 685–700.

Raleigh, C.B., Healy, J.H., Bohn, J., and Bredehoeft, J. 1972. Earthquakes and water flooding in Rangely oil field. Earthquake Notes, **41**: 20–29.

Rebollar, C.J., Kanasewich, E.R., and Nyland, E. 1982. Source parameters from shallow events in the Rocky Mountain House earthquake swarm. Canadian Journal Earth Sciences, **19**: 907–918.

Rebollar, C.J., Kanasewich, E.R., and Nyland, E. 1984. Focal depth and source parameters of the Rocky Mountain House earthquake swarm from digital data at Edmonton. Canadian Journal of Earth Sciences, **21**: 1105–1113.

Rice, J.R., and Cleary, M.P. 1976. Some basic stress diffusion solution for fluid saturated elastic porous media with compressible constituents. Reviews of Geophysics and Space Physics, **14**: 227–241.

Rogers, G.C., and Horner, R.B. 1991. An overview of western Canadian seismicity. *In* Neotectonics of North America. *Edited by* D.B. Slemmons, E.R. Engdahl, M.D. Zoback, and D.D. Blackwell. Geological Society of America, The Geology of North America, Decade Map Volume 1, pp. 69–76.

Rose, M.L. (*Editor*). 1990. The Canadian Society of Petroleum Geologists oil and gas pools of Canada. Series 1, The Canadian Society of Petroleum Geologists, Calgary, Alta.

Segall, P. 1985. Stress and subsidence resulting from subsurface fluid withdrawal in the epicentral region of the 1983 Coalinga earthquake. Journal of Geophysical Research, **B9**: 6801–6816.

Segall, P. 1989. Earthquakes triggered by fluid extraction. Geology, **17**: 942–946.

Simpson, D.W. 1986. Triggered earthquakes. Annual Review of Earth and Planetary Sciences, **14**: 21–42.

Slider, H.C. 1976. Petroleum reservoir engineering methods. Petroleum Publishing Company, Tulsa, Okla.

Smirnova, M.N., Navitskaya, N.A., and Shebalin, N.V. 1975. Earthquake swarm caused by intensive exploitation of an oil field. *In* Proceedings of the 8th International Association of

Seismology and Physics of the Earth Interior General Assembly, Moscow, International Union of Geodesy and Geophysics, Abstracts, p. 39.

Smith, R.B., and Arabasz, W.J. 1991. Seismicity of the Intermountain Seismic Belt. *In* Neotectonics of North America. *Edited by* D.B. Slemmons, E.R. Engdahl, M.D. Zoback, and D.D. Blackwell. Geological Society of America, The Geology of North America, Decade Map Volume 1.

Vanicek, P., and Nagy, D. 1980. Report on the compilation of the map of vertical crustal movements in Canada. Geodynamics Service of Canada, Earth Physics Branch, Open File Report 80-2.

Wetmiller, R.J. 1986. Earthquakes near Rocky Mountain House, Alberta, and their relationship to gas production facilities. Canadian Journal of Earth Sciences, **23**: 172–181.

Yerkes, R.F., and Castle, R.O. 1976. Seismicity and faulting attributable to fluid extraction. Engineering Geology, **10**: 151–167.